ChemComm

COMMUNICATION

View Article Online
View Journal

Cite this: DOI: 10.1039/c8cc03350a

Received 25th April 2018,
Accepted 20th June 2018

DOI: 10.1039/c8cc03350a

rsc.li/chemcomm

Synthesis of zero-valent iron nanoparticles *via* laser ablation in a formate ionic liquid under atmospheric conditions†

Shinya Okazoe,[a] Yoshiro Yasaka,[b] Masaki Kudo,[c] Hiroshi Maeno,[c] Yasukazu Murakami[cd] and Yoshifumi Kimura *[a]

Transition metal nanoparticles (NPs) are promising materials for use as catalysts in many processes, although they are easily oxidized under ambient conditions. In this communication, a novel synthetic method is proposed for producing zero-valent iron (Fe) NPs by laser ablation under atmospheric conditions using the reducing properties of a formate-based ionic liquid solvent. The valence state of Fe was confirmed using X-ray absorption near edge structure (XANES) spectroscopy. The Fe NPs adopt a face centered cubic structure after synthesis, which gradually transforms to a body centered cubic structure after one month. The method can be extended to the synthesis of other transition metal NPs that are easily oxidized.

Among the transition metal nanoparticles (NPs) employed in many fields, those composed of noble metals such as platinum,[1] rhodium,[2] and palladium[3] are widely used as catalysts. The materials are stable under atmospheric conditions and have high catalytic activity. However, the expense of noble metals is a significant drawback in commercial applications. Base metals are much more abundant and are possible substitutes for noble metals. Although base metals are widely used in bulk materials, their use in NPs is not popular. Base metal NPs are easily oxidized at the nanoscale and form an oxidized shell under atmospheric conditions,[4] which reduces activity. If this oxidation can be prevented, the applicability of base metal NPs can be expanded. In this report, we describe the preparation of zero-valent iron (Fe) NPs *via* a method that prevents their nanoscale oxidation.

Fe NPs are used in the dehalogenation of pollutants[5] and the hydrogenation of harmful chemicals.[6] Their magnetic properties also are of interest to physical chemists. Improving the oxidation resistance of Fe NPs is important, because these materials are easily oxidized upon exposure to atmospheric oxygen or water. Fe NPs typically are synthesized and stored under nitrogen or argon to prevent oxidation. For example, Fe NPs have been synthesized by reducing Fe^{3+} with sodium borohydride in solutions that have been deoxygenated by an inert gas.[7] Special treatments also are required to prevent oxidation after preparation. As an example, X-ray diffraction and X-ray absorption spectroscopy samples must be prepared under anaerobic conditions.[7]

Fe NPs have been coated with silicon dioxide to overcome their susceptibility to oxidation.[8] Although this procedure increases resistance to oxidation, the reactive surface is blocked by the protecting layer. In this communication, we produce zero-valent Fe NPs by laser ablation of metallic Fe in an ionic liquid (IL) that provides a reducing environment. Ionic liquids (ILs) are low-melting-point salts composed of organic cations and anions. ILs have unique properties including high ionic conductivity and negligible vapor pressure.[9] The properties of ILs can be modulated by changing their cationic and anionic constituents. We have selected the combination of a phosphonium cation and a formate anion, each of which plays an independent role. The phosphonium cation acts as a stabilizer to prevent nanoparticle aggregation, and the formate anion serves as a reducing reagent. ILs have previously been used to protect metal NPs during syntheses by means of chemical reduction,[10] metal vapor deposition,[11] thermal decomposition,[12] and laser ablation.[13] One of the present authors has reported the synthesis of gold (Au) NPs *via* laser ablation in imidazolium-based ILs.[13a] According to this report, Au NP stability is greater in ILs with longer alkyl chains. Therefore, we have selected the tetraoctylphosphonium ($[P_{8888}]^+$) cation as the protecting agent. The imidazolium cation is not suitable in this instance, because it is unstable in the presence of the formate anion.

[a] *Department of Applied Chemistry, Graduate School of Science and Engineering, Doshisha University, Kyotanabe, Kyoto 610-0321, Japan. E-mail: yokimura@mail.doshisha.ac.jp*
[b] *Department of Molecular Chemistry and Biochemistry, Faculty of Science and Engineering, Doshisha University, Kyotanabe, Kyoto 610-0321, Japan*
[c] *The Ultramicroscopy Research Center, Kyushu University, Fukuoka 819-0395, Japan*
[d] *Department of Applied Quantum Physics and Nuclear Engineering, Kyushu University, Fukuoka 819-0395, Japan*

† Electronic supplementary information (ESI) available: Experimental details and supplemental figures. See DOI: 10.1039/c8cc03350a

Formate was chosen as the IL anion based on its reducing properties and the expectation that it will reduce oxidized Fe NPs. In a previous paper, we demonstrated the reducing capability of formate ions in the synthesis of Au and silver NPs from their corresponding metal ions in formate-containing ILs.[14]

Laser ablation is used to synthesize Fe NPs in this work. Irradiation of the target with a laser pulse locally melts and vaporizes the metal. Some metal atoms in the solution emit electrons and become ionized. Hot metal atoms or cations are cooled by the surrounding medium and form metal NPs. The emitted electrons recombine with cations. Thus, the valence state of the metal does not change upon laser ablation. Zero-valent Fe NPs are easily oxidized, if oxygen or water is present in the solution. In an $[P_{8888}]$HCOO IL, it is expected that oxidized Fe NPs will be reduced by the formate ion or that oxygen and water will be deactivated by the reaction with formate.

Fe NPs were synthesized by ablation with a Nd:YAG laser under ambient conditions using two ILs: tetraoctylphosphonium formate ($[P_{8888}]$HCOO) and tetraoctylphosphonium bis(trifluoromethylsulfonyl)imide ($[P_{8888}]$TFSI). The ILs were evacuated under 1 Pa at 60 °C for 16 h. A schematic illustration of the experimental set-up is shown in Fig. 1. The Fe target was ablated in a vessel filled with the IL. All samples were stored in the atmosphere after preparation. The water content of the Fe colloidal solution was estimated using the ^{1}H NMR signal of water (Fig. S1, ESI†). The water content was 3 mol% (0.1 wt%). Transmission electron microscopy (TEM) images and scanning transmission electron microscopy (STEM) images of Fe NPs were obtained using JEM-3200FSK and JEM ARM200F, respectively. The X-ray absorption near edge structure was measured at BL-12C of the Photon Factory in the fluorescence mode. Details are described in the ESI.†

A TEM image of Fe NPs produced *via* laser ablation in $[P_{8888}]$HCOO and its size distribution histogram are shown in Fig. 2. It was difficult to collect clear lattice images that reveal the atomic arrangement of the Fe NPs due to residual $[P_{8888}]$HCOO, which contributes a significant background to the TEM observations. The NPs are roughly spherical and are composed of Fe which was confirmed by energy dispersive X-ray spectroscopy (EDS). Analyzing the histogram of the size distribution, the average diameter of Fe NPs is found to be 7.1 ± 3.5 nm, here variance is the standard deviation (Fig. 2). This dimension is slightly smaller than the average diameter of NPs prepared in solvents such as water.[15] In Fig. S3 (ESI†), we show the element mapping of Fe, O and P conducted using

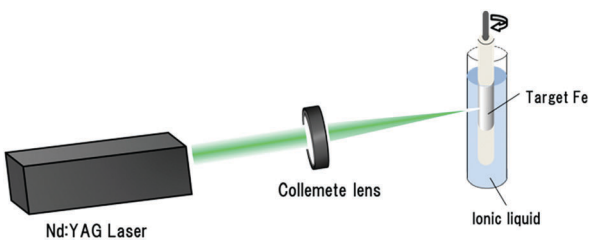

Fig. 1 Schematic illustration of experimental setup. The target Fe foil is rotated during laser ablation.

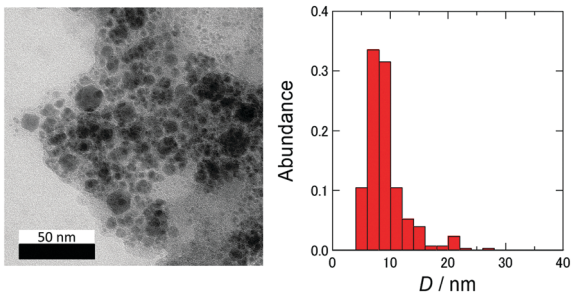

Fig. 2 A TEM image of Fe NPs (left) and the size distribution of NPs (right). The average diameter of Fe NPs was obtained from TEM image, and it was 7.1 ± 3.5 nm.

EDS, together with a high-angle annular dark-field STEM (HAADF-STEM) image. As shown in the figure, the distribution of Fe element overlaps the shape of the STEM image, and the NPs are confirmed to be composed of Fe element. P and O elements derived from the formate IL are also confirmed by the mapping, which cover the Fe NPs. The distribution of oxygen is somewhat broader than that of phosphorus, probably because this image was taken on the grid covered by a holey amorphous carbon film and because of the effect of the adsorbed oxygen on the grid. The results of EDS mapping anticipate that the NPs do not suffer from oxidization.

To clarify the valence, structure, and stability of the synthesized Fe NPs, X-ray absorption near edge structure (XANES) spectra were measured at different times after preparation. Fig. 3 shows the XANES spectra of Fe NPs in ILs one day and one month after preparation and the spectra of the reference substances (Fe foil and α-Fe_2O_3). The Fe foil shows a K-edge signal at 7112 eV, which appears as a shoulder on the first peak at 7131 eV. The α-Fe_2O_3 powder shows a pre-edge peak at 7115 eV and a maximum at 7134 eV. As shown in Fig. 2, the XANES spectrum of Fe NPs in $[P_{8888}]$HCOO one day after preparation differs greatly from those of Fe foil and α-Fe_2O_3. Therefore, the Fe NP structure is different from those of the references. However, the near edge structure (7112 eV) of Fe NPs in $[P_{8888}]$HCOO is quite similar to that of Fe foil,

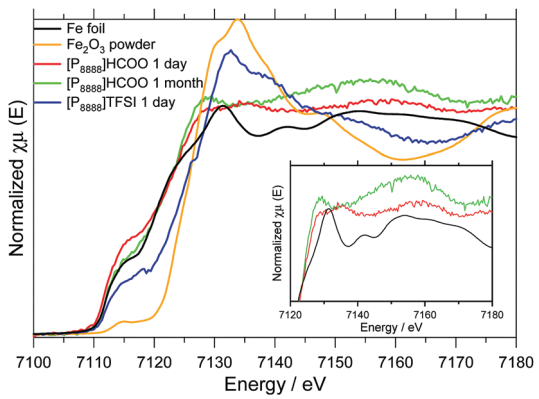

Fig. 3 XANES spectra of reference materials and Fe NPs produced *via* laser ablation in ILs. The inset figure is an enlargement of the Fe and Fe NP in $[P_{8888}]$HCOO spectra over a smaller energy range.

Table 1 Comparison of peak energies from the XANES spectra of Fe nanoparticles prepared *via* laser ablation and of fcc and bcc Fe in the bulk state

	Peak top energy/eV			
Peak number	bcc Fe	fcc Fe[a]	One day after	One month after
First	7134	7128	7130	7129
Second	7142	7136	7135	7156[b]
Third	7153	7160	7158	—

[a] The peak energies of fcc Fe are taken from ref. 16 (C. Marini). [b] This peak corresponds to the second and third peaks of bcc Fe.

which suggests that Fe NPs are not oxidized in $[P_{8888}]HCOO$, although the solution was exposed to air. On the other hand, the X-ray absorption fine structure (XAFS) after the edge clearly differs from that of Fe foil. The Fe NPs in $[P_{8888}]HCOO$ show peaks at 7130, 7135, and 7158 eV, whereas the Fe foil shows peaks at 7134, 7142, and 7153 eV (Table 1).

We noticed that the spectrum of Fe NPs in $[P_{8888}]HCOO$ one day after preparation is very similar to that of fcc Fe. According to ref. 16, fcc Fe produces peaks at 7128, 7136, and 7160 eV (Table 1). Based on this similarity, the freshly prepared NP in $[P_{8888}]HCOO$ is not oxidized and has an fcc structure unlike the typical bcc structure of Fe under ambient conditions. Because Fe NPs produced *via* laser ablation are formed at high temperature and rapidly cooled by the surrounding medium, the particles are quenched in an fcc structure, which is stable at high temperature and pressure. The XANES spectrum of Fe NPs in $[P_{8888}]HCOO$ one month after preparation clearly differs from that one day after preparation, indicating a change in the structure from fcc. Compared with the spectrum one day after preparation, the first peak (7130 eV) is higher and the second peak is absent. The position of the third peak shifts to a lower energy (7156 eV). However, because the intensity of the edge peak at the shoulder is similar to that of the Fe foil, the Fe atoms of Fe NPs in $[P_{8888}]HCOO$ one month after preparation are considered to be unoxidized. The change in the XANES spectrum after the edge is attributed to a partial change in the structure from fcc to bcc. The spectrum is similar to that observed during the bcc to fcc transition of Fe (Fig. 5 in ref. 16). The results reflect the structural instability of Fe NPs and their transformation into a stable structure over time.

The valence state of Fe NPs changes upon changing the anion from $HCOO^-$ to $TFSI^-$. The XANES spectrum of Fe NPs produced in $[P_{8888}]TFSI$ differs from those produced in $[P_{8888}]HCOO$. A small pre-edge peak arising from oxidized Fe is found on the XANES shoulder peak, which points to the oxidation of Fe NPs prepared with $[P_{8888}]TFSI$. The vibrational structure after the pre-edge is very similar to that of α-Fe_2O_3. Therefore, most Fe atoms in Fe NPs produced in $[P_{8888}]TFSI$ are oxidized during preparation or storage, which is consistent with the ability of $HCOO^-$ to protect Fe NPs from oxidation.

Ablation conditions also are important in controlling the valence of Fe NPs. We attempted the synthesis of more concentrated Fe NPs by reducing the volume of $[P_{8888}]HCOO$. Here, the IL was coated on the Fe foil, and laser ablation was conducted as shown in Fig. S4 (ESI†). Because $[P_{8888}]HCOO$ has sufficient viscosity, the IL remains on the surface during ablation. After ablation, the IL-containing Fe NPs were collected, and XANES spectra were obtained at the Fe K-edge. The XANES spectrum of this product, which is shown in Fig. S5 (ESI†), contains a pre-edge peak at 7115 eV and an oscillatory structure after the pre-edge which is similar to that of α-Fe_2O_3. Therefore, Fe NPs produced from thin-coated $[P_{8888}]HCOO$ are oxidized. We think that the depth of the IL solution is an important factor preventing oxidation. In normal ablation, the depth of the interface in contact with air is typically 2 cm. However, the estimated thickness of the coated IL layer is 0.5 mm. During expansion of the Fe droplet produced by the laser pulse, particles may come into contact with air and be oxidized. This process is inhibited in normal ablation. This result indicates that $HCOO^-$ lacks the ability to reduce Fe_2O_3 once it is produced and that residual $HCOO^-$ is present after ablation.

A cyclic voltammogram of $[P_{8888}]HCOO$ in acetonitrile (1 mol kg^{-1}) is shown in Fig. S6 (ESI†). The anodic peak at -1.5 V corresponds to the oxidation of the formate ion based on a comparison of the $[P_{8888}]HCOO$ voltammogram with that of formic acid in aqueous solution.[17] The reaction is described by the following equation:

$$HCOO^- \rightarrow CO_2 + H^+ + 2e^- \quad (1)$$

The broad peak near -0.9 V is attributed to the oxidation of the material on the platinum electrode surface following formate oxidation. The peak also is detected on the negative going scan and is presumed to arise from the oxidation of residual formate. The redox potential of $[P_{8888}]HCOO$ in acetonitrile determined from the more negative voltammetric peak is -0.7 V *versus* the standard hydrogen electrode (SHE) following correction relative to the Ag/Ag^+ potential. A potential of -0.7 V is sufficient to reduce oxidized Fe, because Fe ions are reduced at 0.44 V *versus* SHE. However, oxidized NPs are not reduced by the formate ion in the experimental system. There are two plausible reasons for this. One is that the oxidation potential of the neat IL is not as negative as that of the IL diluted in acetonitrile. Another is that the Fe_XO_Y redox potential in NPs is not the same as that of bulk Fe^{2+}. At present, we do not have an explanation for the observed behavior.

The success in forming zero-valent Fe NPs likely depends on the efficient reaction of the formate ion with oxygen dissolved in the IL, which prevents the oxidation of Fe. The proposed reaction scheme is shown in eqn (2).

$$2HCOO^- + O_2 \rightarrow 2HCO_3^- \quad (2)$$

In summary, we have demonstrated a new synthetic method for preparing zero-valent Fe NPs under atmospheric conditions. The procedure for producing Fe NPs that are resistant to oxidation involves simple laser pulse irradiation of a Fe foil target immersed in $[P_{8888}]HCOO$. The method can be extended to the preparation of other easily oxidizable transition metal NPs.

This work is supported by a fund from the AMADA FOUNDATION (AF-2015210) and partially by a fund from the MEXT-Supported Program for the Strategic Research Foundation at Private Universities 2015–2019 (S1511025). TEM observations were performed as part of a program conducted by the Advanced Characterization Nanotechnology Platform sponsored by the MEXT, Japan. XANES measurements were supported by the Photon Factory Program Advisory Committee (Proposal No. 2017G564). S. O. and Y. K. thank Prof. Sakae Takenaka (Doshisha University) and Prof. Hiroshi Kitagawa (Kyoto University) for the helpful discussion.

Conflicts of interest

There are no conflicts to declare.

Notes and references

1 (*a*) Z. Peng and H. Yang, *Nano Today*, 2009, **4**, 143; (*b*) S. Guo, S. Zhang and S. Sun, *Angew. Chem., Int. Ed.*, 2013, **52**, 8526.
2 (*a*) S. K. Singh, X.-B. Zhang and Q. Xu, *J. Am. Chem. Soc.*, 2009, **131**, 9894; (*b*) N. Yan, Y. Yuan and P. J. Dyson, *Chem. Commun.*, 2011, **47**, 2529; (*c*) Q. Yao, Z.-H. Lu, Y. Jia, X. Chen and X. Liu, *Int. J. Hydrogen Energy*, 2015, **40**, 2207.
3 (*a*) X. Chen, G. Wu, J. Chen, X. Chen, Z. Xie and X. Wang, *J. Am. Chem. Soc.*, 2011, **133**, 3693; (*b*) H. Wu, H. Li, Y. Zhai and Xi. Xu and Y. Jin, *Adv. Mater.*, 2012, **24**, 1594.
4 (*a*) X. Song, S. Sun, W. Zhang and Z. Yin, *J. Colloid Interface Sci.*, 2004, **273**, 463; (*b*) N. Lasemi, U. Pacher, C. Rentenberger, O. B. Miguel and W. Kautec, *Chem. Phys. Chem.*, 2017, **18**, 1118.
5 B. C. Reinsch, B. Forsberg, R. L. Penn, C. S. Kim and G. V. Lowry, *Environ. Sci. Technol.*, 2010, **44**, 3455.
6 (*a*) J. Xu, S. A. Baig, X. Lv and X. Xu, *J. Hazard. Mater.*, 2013, **244–245**, 628; (*b*) C. B. Wang and W. X. Zhang, *Environ. Sci. Technol.*, 1997, **31**, 2154.
7 Y. P. Sun, X. Q. Li, W. X. Zhang and H. P. Wang, *Colloids Interface Sci. A: Eng. Aspects*, 2007, **308**, 60.
8 S. Yamamoto, G. Ruwan, Y. Tamada, K. Kohara, Y. Kusano, T. Sasano, K. Ohno, Y. Tsuji, H. Kageyama, T. Ono and M. Takano, *Chem. Mater.*, 2011, **23**, 1564.
9 (*a*) H. Tokuda, K. Hayamizu, K. Ishii, M. A. B. H. Susan and M. Watanabe, *J. Phys. Chem. B*, 2004, **108**, 16593; (*b*) H. Tokuda, K. Hayamizu, K. Ishii, M. A. B. H. Susan and M. Watanabe, *J. Phys. Chem. B*, 2005, **109**, 6103.
10 (*a*) M. Migowski, D. Zanchet, G. Machado, M. A. Gelesky, S. R. Teixeira and J. Dupont, *Phys. Chem. Chem. Phys.*, 2010, **12**, 6826; (*b*) K. L. Luska and A. Moores, *Green Chem.*, 2012, **14**, 1736; (*c*) J. Dupont and J. D. Scholten, *Chem. Soc. Rev.*, 2010, **39**, 1780.
11 (*a*) T. Torimoto, K. Okazaki, T. Kiyama, K. Hirahara, N. Tanaka and S. Kuwabata, *Appl. Phys. Lett.*, 2006, **89**, 243117; (*b*) E. Vanecht, K. Binnemans, S. Patskovsky, M. Meunier, J. W. Seo, L. Stappers and J. Fransaer, *Phys. Chem. Chem. Phys.*, 2012, **14**, 5662.
12 (*a*) S. Wegner and C. Janiak, *Top. Curr. Chem.*, 2017, **375**, 65; (*b*) C. Janiak, *Z. Naturforsch., B: J. Chem. Sci.*, 2013, **68**, 1059.
13 (*a*) Y. Kimura, H. Takata, M. Terazima, T. Ogawa and S. Isoda, *Chem. Lett.*, 2007, **36**, 1130; (*b*) H. Wender, M. L. Andreazza, R. R. B. Correia, S. R. Teixeira and J. Dupont, *Nanoscale*, 2011, **3**, 1240; (*c*) M. A. Gelesky, A. P. Umpierre, G. Machado, R. R. B. Correia, W. C. Magno, J. Morais, G. Ebeling and J. Dupont, *J. Am. Chem. Soc.*, 2005, **127**, 4588; (*d*) H. P. S. Castro, V. S. Souza, J. D. Scholten, J. H. Dias, J. A. Fernandes, F. S. Rodembusch, R. D. Reis, J. Dupont, S. R. Teixeira and R. R. B. Correia, *Chem. – Eur. J.*, 2016, **22**, 138.
14 S. Okazoe, Y. Yasaka, M. Ueno and Y. Kimura, *Chem. Lett.*, 2017, **46**, 1344.
15 V. Amendola, M. Meneghetti, G. Granozzi, S. Agnoli, S. Polizzi, P. Riello, A. Boscaini, C. Anselmi, G. Fracasso, M. Colombatti, C. Innocenti, D. Gatteschid and C. Sangregoriode, *J. Mater. Chem.*, 2011, **21**, 3803.
16 C. Marini, F. Occelli, O. Mathon, R. Torchio, V. Recoules, S. Pascarelli and P. Loubeyre, *J. Appl. Phys.*, 2014, **115**, 093513.
17 J. John, H. Wang, E. D. Rus and H. D. Abruña, *J. Phys. Chem. C*, 2012, **116**, 5810.

